Heat-capacity study of the second layer of ^{3}He adsorbed on Grafoil

S. W. Van Sciver* and O. E. Vilches
Department of Physics, University of Washington, Seattle 98195
(Received 19 December 1977)

Heat-capacity measurements on adsorbed ^{3}He are reported. The densities studied start slightly under monolayer completion and go up to slightly above second-layer completion. The temperature range is 0.04 K $< T <$ 4.2 K. After subtraction of calculated values of the contributions from the first layer (solid), and desorption, we find that the second layer behaves as a two-dimensional interacting Fermi gas at all densities for which a partial third layer is not present. The second-layer gas cannot be represented by the same second virial coefficient used for the first layer. The absence of the substrate-induced ordering transition allows one to study the gas behavior over a larger range of densities than on the first layer. We find that the shape, temperature, and density dependence of the very low temperature ($\sim$0.1 K) rounded anomaly in the specific heat is different than on the first layer. With a very small amount of third layer present, the second layer solidifies for temperatures below 0.98 K.

I. INTRODUCTION

Monolayer films of ^{3}He, ^{4}He, and ^{3}He-^{4}He mixtures adsorbed on graphite show distinct phases that to considerable accuracy can be described by two-dimensional models.[1] These phases were first surveyed[2,3] in calorimetric and vapor-pressure studies, but NMR[4-8] and neutron-scattering[9,10] results on the same adsorbing substrate have become available. These results have confirmed to a great extent the model-aided conclusions derived from the heat-capacity studies. In particular, they have shown fluid behavior at low densities or high temperatures, the existence of the substrate registered phase, and solid behavior and melting at high densities.

Multilayer films of ^{4}He on the same substrate have also been experimentally studied.[11-14] These studies have addressed two distinct problems: (i) the behavior of the second adsorbed layer and (ii) multilayer films and the onset of bulk behavior. No complete study of multilayer ^{3}He films adsorbed on graphite has been made, although indications of mobile behavior for the second layer have been found in the NMR (Ref. 7) and neutron-scattering studies.[10] In this paper we report a systematic heat-capacity study of ^{3}He adsorbed on Grafoil,[15] for densities varying from that of a completed monolayer up to that corresponding to slightly more than a completed second layer. In a following paper,[16] one of us (SVS) describes measurements carried out with films at densities corresponding to more than two layers. A preliminary report of some of the results presented here was given previously.[17]

II. EXPERIMENTAL

The techniques used for measuring the heat capacity of helium films adsorbed on Grafoil have been discussed in detail in previous papers.[2] The heat capacity of the empty calorimeter or calorimeter plus adsorbed helium is obtained by supplying a known heat pulse (ΔQ) and measuring the change in the equilibrium temperature (ΔT). The film heat capacity is the difference between the heat capacities of the loaded and empty calorimeter.

The measurements were carried out using a dilution refrigerator to cool the adsorption cell to about 40 mK. The highest temperature where temperature drifts were not excessive was about 4 K. The adsorption cell had an Evanohm heater, a cerium-magnesium-nitrate (CMN) magnetic thermometer for use below 1.5 K, and two carbon resistance thermometers (see Fig. 1 of Ref. 2). The adsorption cell was cell B of Ref. 2. Approximately 62.5 cm^3 STP of ^{4}He and 63.5 cm^3 STP of ^{3}He are required for the critical "$\frac{1}{3}$" ordered structure.

Samples were prepared in a gas handling system consisting of a calibrated volume V and a Baratron capacitance gauge. The amount of adsorbed gas was determined, using the ideal-gas law, from the temperature of the calibrated volume V and the initial and final pressures (before and after adsorption). The ^{3}He used in the study was 99.9% pure as received.

Throughout this paper we will call n the ratio of the total number of particles adsorbed in the cell to the area of the substrate as determined by multiplying the number of ^{4}He atoms at critical "$\frac{1}{3}$" coverage (see Sec. III A) by three times the area of a graphite hexagon (5.236 Å^2). For coverages below a monolayer, n is then the areal density. For coverages above a monolayer, n is only a convenient way of expressing the total number of particles in the cell. The actual areal density of the first and second layers will be called, respectively, n_1 and n_2.

III. SECOND-LAYER STUDY

The prime reason for doing this study was to look at how the different substrate [solid two-dimensional (2-D) ^{3}He instead of graphite] affected the behavior of the monolayer (actually second-layer) film. A large drop in the 2-D condensation temperature of second-layer ^{4}He as compared to the first-layer was found by Bretz and Polanco.[14] An apparent increase in the condensation temperature has been found on ^{4}He films adsorbed on argon-plated Grafoil,[18,19] and a decrease with a substrate of Ne-plated Grafoil.[20] Although ^{3}He is not believed to condense in two dimensions,[21] there is a rounded anomaly in the heat capacity at $T \simeq 0.1$ K whose origin (and consequently substrate dependence) is unknown. We precede the presentation of our results by a brief review of the monolayer-^{3}He results.

A. Submonolayer review

The complete phase diagram for the first atomic layer of ^{3}He is shown in Fig. 1. Three regions are clearly distinguishable. Below about $n = 0.06$ Å^{-2}, the film is seen to behave as a 2-D gas. The specific heat per atom is close to k (Boltzmann's constant) at temperatures above 2 K, and drops off monotonically toward zero at lower temperature. Near 0.1 K a shoulder in the heat capacity is seen which is believed to be due to ^{3}He-^{3}He

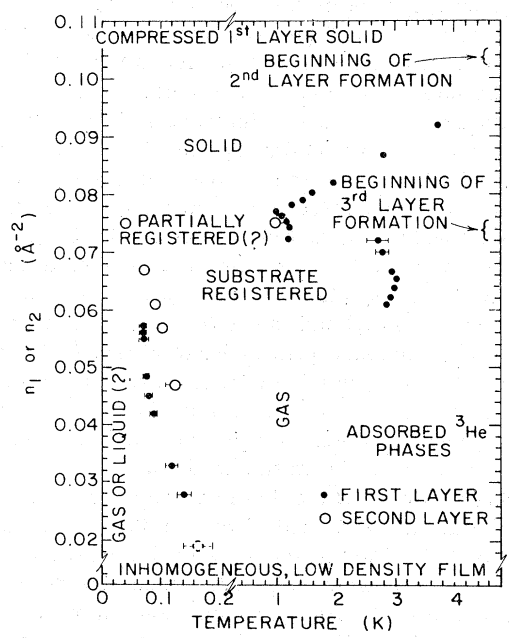

FIG. 1. Density vs temperature at which anomalies in the heat capacity occur for both first-layer (●) and second-layer (○) ^{3}He films. Identification of phases correspond to the first-layer measurements.

interactions. A theoretical description by Siddon and Schick[22] treats the film as a gas of interacting helium atoms which are constrained to move in two dimensions. Deviations from ideality are considered in terms of the quantum virial expansion. If the expansion can be truncated after quadratic terms, the heat capacity will have the form

$$C = Nk\left(1 - n\beta^2 \frac{d^2B}{d\beta^2}\right), \tag{1}$$

where B is the second virial coefficient, $\beta = 1/kT$, and N is the total number of adsorbed atoms. Comparison between the data and the theory when B is calculated using the Lennard-Jones or the Beck[23] potentials to describe He-He interactions has shown rather good agreement for temperatures above 0.5 K.

At intermediate densities, the specific-heat signal changes drastically with a small increase in density. A sharp peak near 3 K is seen at the density for which there is one helium atom for every three graphite adsorption sites.[2,24] The transition identifies the critical coverage for the helium atoms to form a regular array commensurate with the substrate (called $x_g = \frac{1}{3}$ in previous heat capacity studies,[2] or $\sqrt{3} \times \sqrt{3}$ in diffraction work).

From $n = 0.078$ Å^{-2} to layer completion the film has properties attributable to a 2-D solid. Two features in the experimental heat-capacity identify this phase: (i) melting peaks that correlate well in temperature with the melting temperatures of bulk ^{3}He for similar interatomic spacings, and (ii) low temperature T^2 dependence of the heat capacity which give Debye temperatures similar to those obtained in three dimensions. Measurements of relaxation times with pulsed NMR have found essentially the same melting line,[8] while neutron scattering measurements have shown the solid to have a triangular lattice structure incommensurate with the substrate.[10]

In a narrow density range before the start of the 2-D solid, a new phase that resembles the $\sqrt{3} \times \sqrt{3}$ critical region has been observed.[25] Apparent critical coverage and densities are $n_c = 0.074$ Å^{-2} and $T_c = 1.23$ K. The exact nature of this phase is still not known, but it has been suggested[26] that it could be due to a coexistence of the $\sqrt{3}$ and solid phases.

B. Second-layer study – general

As the first monolayer is completed, deviations are observed from the low temperature T^2 behavior characteristic of a 2-D solid, Fig. 2. The increase in the specific heat is due to a fraction of the atoms of the film being on the second layer

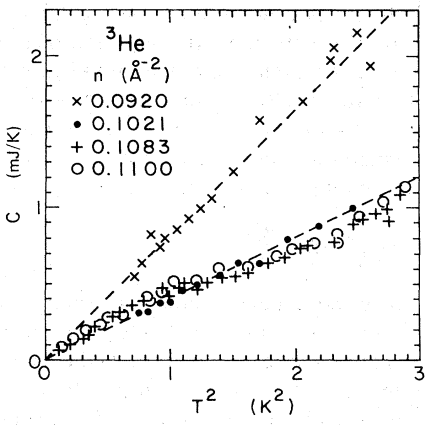

FIG. 2. Total measured heat capacity of various films adsorbed on our calorimeter through monolayer completion.

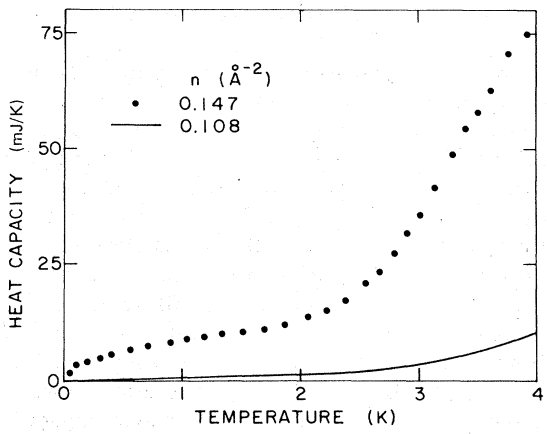

FIG. 3. Total measured heat capacity of one two-layer film ($n = 0.1466$ Å^{-2}). Solid line is the heat capacity of a film at monolayer completion.

where they again start having large mobility and giving gas-type heat capacities. Before monolayer completion ($n = 0.092$ and 0.102 Å^{-2}) the Debye temperatures of the 2-D solid increase rapidly with density (see also Fig. 7 of Ref. 25). On the other hand, the runs at $n \cong 0.108$ and 0.110 Å^{-2} appear almost insensitive to coverage. We believe this is due to the high compressibility of the first-layer solid. As more atoms are added, some go to the first layer increasing its density (and its Debye temperature). The signal for the underlying first layer in Fig. 2 would then be a straight line of smaller slope than the ones shown. The more helium one adds to the second layer, the smaller the contribution becomes from the first layer. The total contribution to the heat capacity from the second layer atoms in run $n = 0.1100$ Å^{-2} is then larger than the contribution for the $n = 0.1083$ Å^{-2} run. We have not pursued looking at first-layer completion in more detail to see if there is an abrupt change from the purely 2-D solid regime to the 2-D solid-plus-mobile-atoms behavior as seems to be indicated by the NMR results.[7,8] Later in this section we show that another calorimetric study indicates that monolayer completion occurs over a range of coverages.

Our second-layer measurements have been done at $n \cong 0.110$, 0.129, 0.136, 0.147, 0.157, 0.167, 0.171, 0.178, and 0.186 Å^{-2}, for $0.04 < T < 4.2$ K. An example of the raw data over the full temperature range for an intermediate density $n = 0.147$ Å^{-2} is shown in Fig. 3. For comparison, the smooth line representing the heat capacity of the $n = 0.108$ Å^{-2} run is also shown. If we assume that the smooth line approximately corresponds to the heat capacity of the first layer in the $n = 0.147$ Å^{-2} film, then the total signal has two gross features. Below 1.5 K it is a relatively flat monotonic function of temperature that drops off toward zero at the lowest temperatures. Above 1.5 K, there is a steep rise. This rise occurs at the same T at which we observed an increase in the equilibrium three-dimensional (3-D) pressure in the cell.

We have developed a model for the various contributions to the signal shown in Fig. 3 and to the heat capacity of the other densities that we measured, except the higher ones. A relatively flat heat capacity that drops almost linearly to zero at lower temperatures is indicative of a gas-type behavior. A fast rise in the heat capacity coupled with an increase in the vapor pressure indicates desorption of the film. Our model assumes that the total measured heat capacity is the sum of five independent contributions: the calorimeter, a solid first layer, a 2-D interacting Fermi gas, a 3-D vapor, and film desorption. The calorimeter contribution is constant throughout the measurement, was measured in an independent run, and has already been subtracted out in Fig. 3. To calculate the other contributions we need to know at every temperature the amount of ^{3}He in the 3-D vapor phase (N_v) and in the film (N_f), and then divide the amount adsorbed into a first (N_1) and a second (N_2) layer ($N_1 + N_2 = N_f$). Vapor pressure measurements were taken in conjunction with the heat-capacity measurements at some selected temperatures. From the dead volumes in our system (8.33 cm^3 inside the calorimeter cell, 0.27 cm^3 at 4.2 K, and 27 cm^3 at 300 K) we calculated N_v. Furthermore, we divided N_v into $N_v = N_{lv} + N_{hv}$, where N_{lv} is the vapor inside the calorimeter, while N_{hv} is the vapor in the rest of the system. Knowing the total amount of gas put into the system (N) the amount in the film is $N_f = N - N_v$.

The separation of N_f into N_1 and N_2 required a

more detailed analysis due to the compressibility of the first layer. Our own heat-capacity measurements extend to 4 K. Elgin, Goodstein, and Greif[27] have measured the heat capacity and vapor pressure of monolayer and multilayer films of ^{3}He at selected temperatures between 2.41 and 19.6 K to construct a complete set of thermodynamic data as was done previously[3] for ^{4}He. The temperature interval between their data points is approximately 0.3 K at the lower temperatures and larger at higher temperatures. Their data are tabulated as a function of N_f. It is easy to use the $\frac{1}{3}$ ordering transition in a monolayer to correlate their data with ours. When this is done, the melting peaks observed by Hering *et al.*[25] and those measured by Elgin *et al.* fall on a continuous line, Fig. 4(a) within the error in the determination of T_{peak}. Fig. 4(a) shows that as the first layer is completed the melting peak temperature increases linearly with coverage up to $n_f \cong 0.104$ Å^{-2}. Above $n_f \approx 0.120$ the peak temperature increases only slightly with temperature. We have assumed that the straight line drawn through the $n_f < 0.104$ Å^{-2} peak temperatures can be extrapolated to higher densities to represent the actual first-layer density for that melting temperature. The straight line is used to calculate n_1 (and N_1) from a given value of n_f (or N_f). Our $n = 0.147$ run is at a coverage slightly larger than the one of the highest peak in Elgin, Goodstein, and Greif's data, but a smooth straight line was drawn through their last three points. The procedure is illustrated in Fig. 4(a). As N_f gets depleted at higher temperatures due to desorption, n_f decreases and so do n_1 and n_2.

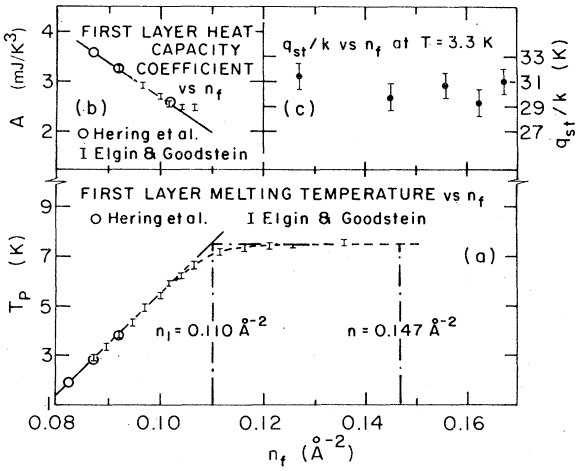

FIG. 4. Various parameters used in the calculation of first- and second-layer coverages and heat capacities as a function of n_f. (a) First-layer melting temperature (from Refs. 25 and 27). (b) First-layer heat-capacity coefficient A (Eq. 2). (c) Isosteric heat at $T = 3.3$ K.

With the calculated values of N_{iv}, N_1, and N_2, the various contributions to the heat capacity were calculated in the following way.

(i) First layer: Hering *et al.* noted that the heat capacity of the first-layer solid could be well represented by $C = 3.6(T^2/T_p)$ mJ/K^2 for coverages between 0.078 and 0.087 Å^{-2} (Fig. 10 of Ref. 24). We have found (again by combining our own data with those of Ref. 27) that for higher coverages, deviations occur with the coefficient decreasing with coverage in an approximate linear fashion, Fig. 4(b). We have represented the first-layer contribution to the heat capacity by

$$C_1 = A(T^2/T_p) \tag{2}$$

and for the calculation have taken A from the straight line of Fig. 4(b) and T_p from Fig. 4(a).

(ii) Second layer: This contribution is not known, in fact being the object our of measurement. Since for these lower densities its contribution appears to be that of a 2-D gas, we approximated its value by Siddon and Schick's[21,22] calculated heat capacity for a 2-D ^{3}He interacting gas

$$C_2 = N_2 k\left(1 - n_2\beta^2 \frac{d^2B}{d\beta^2}\right),$$

where the values of $B^2(d^2B/d\beta^2)$ were taken from Table III of Ref. 22.

(iii) Vapor: The 3-D vapor was assumed to be an ideal gas, so $C_v = \frac{3}{2}N_{iv}k$. Only N_{iv} was used since although desorption occurs into the entire system, only N_{iv} atoms are heated during the short time it takes to obtain a heat-capacity point.

(iv) Desorption: At higher temperatures, part of the heat goes into evaporating the adsorbed film. The heat-capacity contribution from this process is given by[1]

$$C_D = kT\left(\frac{q_{st}}{kT} - 1\right)\left(\frac{dN_v}{dT}\right)_{eq}, \tag{3}$$

where q_{st} is the isosteric heat of adsorption, and the change in the number of particles is taken along the film vapor equilibrium line. The isosteric heat can be calculated from extensive vapor-pressure measurements as

$$q_{st} = kT^2\left(\frac{\partial \ln P}{\partial T}\right)_{N_f, A}, \tag{4}$$

where P is the 3-D pressure.

An approximate value can be obtained from our small number of vapor-pressure measurements. Since $P \simeq P_0 e^{-q_{st}/kT}$, a plot of $\ln P$ vs $1/T$, corrected to constant coverage, will yield q_{st}/k. The values we obtained at 3.3 K are plotted in Fig. 4(c). Our experimental system is such that at somewhat lower temperatures (and low pressures, $p < 1$

Torr) thermomolecular corrections are very large, while at higher temperatures there is a considerable depletion of the number of atoms on the adsorbed film. Our estimate gives $q_{st}/k \cong 30.5 \pm 1$ K at 3.3 K for $n = 0.147$. The true isosteric heat is a function of temperature and density. The temperature dependence is approximately as $q_{st} = U_0 + \frac{3}{2}kT$, where U_0 is the binding energy at $T = 0$ K. This variation will introduce a maximum 5% error in C_D in the temperature range in which C_D is important. In view of the large error bar in our q_{st} value, this dependence was ignored in the calculation of C_D. The quantity $(\Delta N_v/\Delta T)_{eq}$ was obtained from our vapor-pressure measurement.

The data, all the contributions, and the sum of all the contributions are plotted in Fig. 5 for $n = 0.147$ Å^{-2}. The agreement between calculation and experiment is very good between 1.4 and 3.4 K, and not too good above or below these temperatures. We believe a smaller temperature-interval set of vapor-pressure measurements would correct the high-temperature discrepancy. The general tendency to "bend down" because of layer depletion is duplicated, but the absolute value is not right. On the low-temperature end, it is obvious that the virial expansion of Siddon and Schick is not adequate to describe the second-layer film. Furthermore, using the actual first-layer data[2] for similar density brings the calculated value closer to the experimental measurement, but not quite in agreement either.

Figure 5 is then useful in determining that we have approximately the right values for C_1 and C_d, that C_v is not important in analyzing the low-temperature data, and that the second layer of ^{3}He behaves as a 2-D interacting Fermi gas.

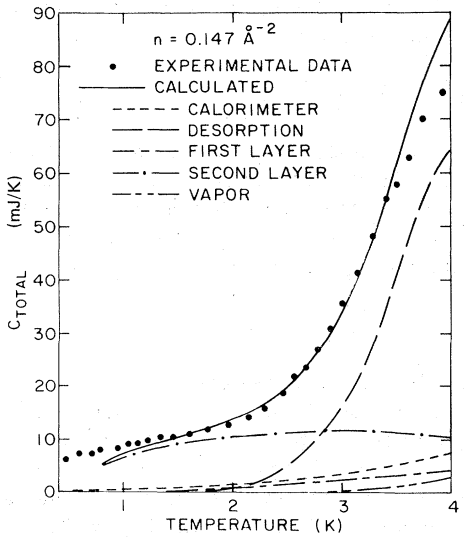

FIG. 5. Comparison between measured and calculated total heat capacity for $n = 0.147$ Å^{-2}.

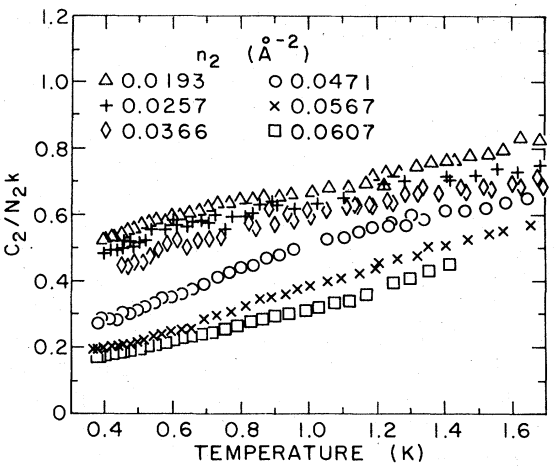

FIG. 6. Second-layer specific heat vs temperature for temperatures above 0.3 K (see text).

C. Second layer below 1.5 K

The second-layer data for densities up to $n_2 = 0.0670$ extracted in the form described in Sec. II is shown in Figs. 6 and 7. Figure 6 shows the data above 0.3 K, while Fig. 7 shows the data below 0.3 K. Both sets were taken in separate runs. For the high-temperature measurements the calorimeter cell was thermally cooled by the supporting nylon tube, while for the low-temperature measurements a superconducting heat switch was added. The heat switch introduced uncertainties in the measurements above 0.4 K due to fast thermal relaxation times, especially at the lower densities. We tried to duplicate as well as possible the coverages of the two sets of data, but for

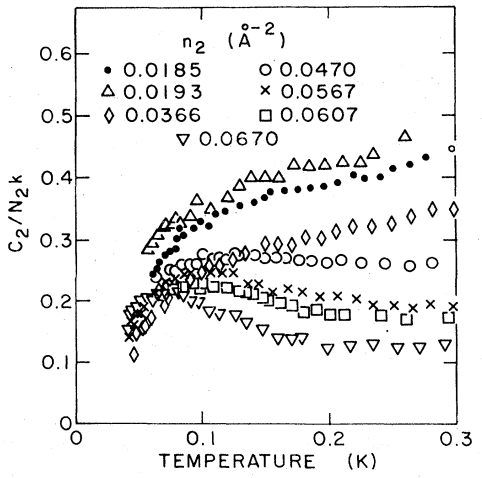

FIG. 7. Second-layer specific heat vs temperature for temperatures below 0.3 K (see text).

some of them, small differences resulted.

On first inspection, it is quite clear that the second layer behaves qualitatively in the same way as the first layer (see, for example, Fig. 9 of Ref. 2). The specific heat shows the interacting Fermi gas behavior down to $T \simeq 0.4$ K, and then has a shoulder around 0.1 K. This shoulder is somewhat different from the one on the first layer. While on the first layer it disappears with increasing coverage at a constant temperature of about 0.07 K, here it gets more pronounced and moves rapidly to lower temperatures. The last full peak we measured occurs at $T \cong 0.07$ K. The location of these peaks as a function of temperature is shown in Fig. 1. There might be one more sharp peak at $T \simeq 0.04$ K and $n_2 \simeq 0.077$ Å^{-2} (see Sec. III D).

We have compared the data above 0.3 K to the calculated specific heat for an interacting Fermi gas and to the first-layer data. Results are shown in Fig. 8 where we have plotted $(C_2/N_2k - 1)n_2^{-1}$ vs T. Since the expression on the left-hand side is independent of coverage[22] [see Eq. (1)], all data should follow a universal curve. From Fig. 8 it is apparent that although the data follow approximately a unique curve for a range of densities comparable to that for which a universal curve is followed on the first layer, the second-layer data do not follow the same universal curve described by the theory or the first-layer data. For comparison of the type of deviation expected at lower densities, we included in the figure a line obtained from data of Hering[28] at $n_1 = 0.0220$ Å^{-2}. These low-density deviations, perhaps unexpected since the virial expansion should be more accurate at low density, are due to the effect of inhomogeneities in the substrate that are not "plated out" by adding one layer of solid ^{3}He.

The overall deviation at higher densities must be due to the different substrates, and to possible Z-wise motion of the ^{3}He atoms on the second layer. This type of motion has been studied for ^{4}He on a two-layer film.[14,29,30] The net effect is a reduction of the attraction between ^{4}He atoms that results in a lowering of the condensation temperature of the 2-D film. For ^{3}He presumably there is no condensation, even on the first layer, but a reduction of the interaction between ^{3}He atoms would tend to make it a more ideal gas, with C_2/N_2k closer to 1. No theoretical calculations of this effect have been made for ^{3}He.

We note that the region of gas-like behavior is much larger on the second layer than on the first due to the absence of the $\frac{1}{3}$ registry transition. The highest coverage shown in Fig. 7 would have corresponded to a coverage higher than the ordering transition on the first layer.

D. Completion of second layer

The 2-D gas signals discussed in Sec. III C end at about $n_2 \simeq 0.074$ Å^{-2}. Figure 9 shows two coverages closely spaced in density, $n_2 = 0.0725$ and $n_2 = 0.0754$ Å^{-2}. These second-layer densities have been obtained by assuming the first layer to be a solid of density $n_1 = 0.1110$ Å^{-2}. While the lower-coverage film shows a heat capacity following the trend of Fig. 5, the higher-density film shows a peak at $T \simeq 0.98$ K, similar in shape to those observed at slightly higher temperature and density when the first-layer solid melts. In fact, within the uncertainties of coverage inherent in this second-layer study, the $n_2 = 0.0754$ Å^{-2} peak appears to lie on an extension of the melting line

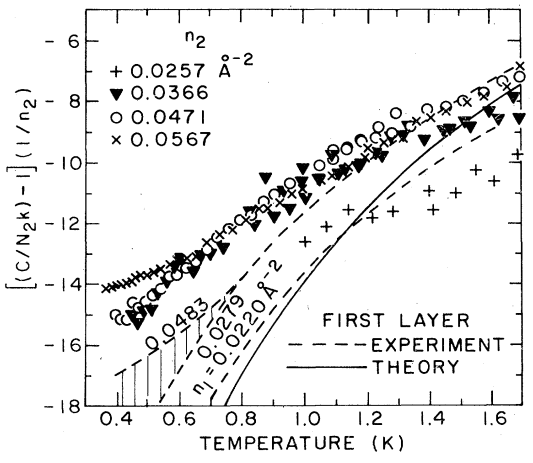

FIG. 8. Comparison of second-layer low-density measurement to similar measurements on the first layer and to theory (Ref. 22).

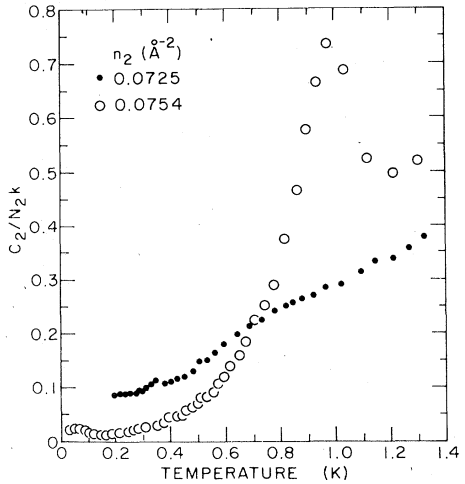

FIG. 9. Specific heat vs temperature at second-layer completion.

of the first-layer solid (see Fig. 1). First-layer melting is not observed at this low density; instead a partially registered phase, or a coexisting solid-$\frac{1}{3}$ ordered phase is seen. Below the peak the heat capacity drops rapidly, but lacks the characteristic T^2 dependence of a 2-D Debye solid. A minimum in the signal is noticeable at 0.15 K, followed by a rise with a maximum at about 0.04 K, just the limit of our temperature range. While this maximum could be due to the same phenomena observed at lower densities, we believe it is due to something occurring on the third layer.[16] So our conclusion is that the second layer will solidify just at second-layer completion or when a very small amount of ^{3}He is present on the third layer. This second-layer solid is rather compressible, so addition of more ^{3}He not only gives more third-layer signal, but also increases the second-layer density and its melting temperature. For a density that would correspond to $n_2 = 0.0845$ Å^{-2}, T_{peak} has shifted to 1.07 K, representing an actual increase of the true n_2 of approximately 0.0015 Å^{-2}. These data are plotted as Fig. 1 of Ref. 16. How melting is affected by the addition of more ^{3}He and the actual evolution of the multilayer signal are also discussed in Ref. 16.

An estimate of the excess signal above two layers, and by subtraction an estimate of second-layer density, can be obtained by using (2) on the second layer. At low densities and for the first layer, $A = 3.6$ mJ/K^2 (Ref. 25). Using the same coefficient for the second layer and $T_p = 0.98$ K, we can generate an effective second-layer heat capacity as shown in Fig. 10. The excess signal (except for the low-temperature peak) is almost parallel to the second-layer solid line, signaling a temperature-independent contribution. For a 2-D ideal gas, $C = Nk$. Assuming the excess signal to be that of an ideal gas, $n_3 \simeq 0.0008$ Å^{-2} leaving the second-layer density at 0.0746 and the total density at $n \simeq 0.186$ Å^{-2} for second-layer completion. This value is in reasonable agreement with the value of 0.181 Å^{-2} we deduced from Elgin *et al.* isotherm data.[27]

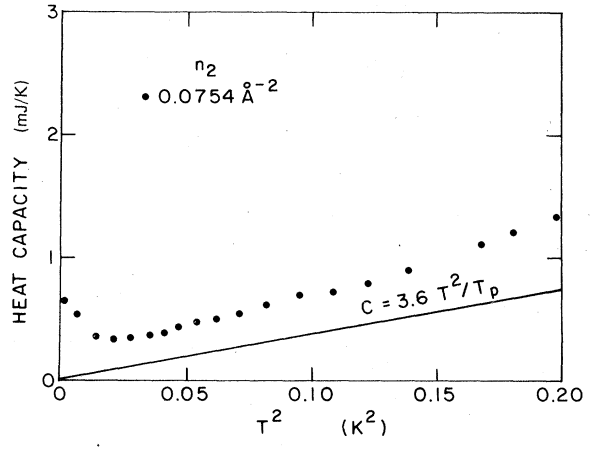

FIG. 10. Low-temperature heat capacity vs temperature at second-layer completion. Solid line is calculated second-layer heat capacity for a 2-D solid with melting temperature $T_p \cong 0.98$ K using Eq. (2).

IV. CONCLUSION

The second layer of adsorbed ^{3}He on Grafoil shows the behavior of an interacting 2-D Fermi gas essentially at all densities above those affected by inhomogeneities in the adsorbing substrate. The behavior is different from that of the first-adsorbed layer due to the different substrate, motion perpendicular to the substrate, and the absence of the $\frac{1}{3}$ ordering transition. We had to model the first layer as a 2-D solid, and subtracted that contribution from the total data to obtain the second-layer signal. Our model is not accurate, but small differences in the density of the first layer will not alter substantially the absolute magnitude of the second-layer contribution, since the first-layer portion is only a small part of the total signal at temperatures below 1 K. The absence of the $\frac{1}{3}$ transition allows one to follow the low-temperature ($T \simeq 0.1$ K) rounded peak of the heat capacity to higher densities and lower temperatures. Although this "line" of second-layer peaks resembles the high-density part of a liquid-vapor coexistence curve (see Fig. 1), theoretical estimates of the 2-D ^{3}He binding energy predict a not-self-bound liquid at $T = 0$. Our data, at present, cannot determine the nature of the very low-temperature phase of adsorbed ^{3}He. No critical point has been found, but inhomogeneities play a very important role for densities up to at least a quarter of a monolayer, the region where the critical point should be if our peaks are part of a coexistence curve. We believe that the second layer becomes solid at or slightly above the density for which a third layer begins to form.

ACKNOWLEDGMENTS

We would like to thank J. G. Dash and M. Schick for many valuable discussions. S. V. Hering, S. B. Crary, and T. M. Chung provided assistance and ideas during the measurements and discussions. A large part of our analysis could not have been carried out without the tables of data of the Caltech group. We are extremely grateful to

R. L. Elgin and D. L. Goodstein for their generosity in providing us with the results of both their measurements and their analysis long before publication. One of us (O.E.V.) thanks M. Bretz for valuable discussions and an early copy of Bretz and Polanco's second-layer ^{4}He results. This work was supported by NSF Grant No. DMR 72 03003 A04.

---

*Present address: Engineering Research Building, University of Wisconsin, Madison, Wis. 53706.

[1]J. G. Dash, *Films on Solid Surfaces* (Academic, New York, 1975).
[2]M. Bretz, J. G. Dash, D. C. Hickernell, E. O. McLean, and O. E. Vilches, Phys. Rev. A 9, 2657 (1974).
[3]R. L. Elgin and D. L. Goodstein, Phys. Rev. A 9, 2657 (1974).
[4]R. J. Rollefson, Phys. Rev. Lett. 29, 410 (1972).
[5]S. G. Hegde, E. Lerner, and J. G. Daunt, Phys. Lett. A 49, 437 (1974); D. C. Hickernell, D. L. Husa, and J. G. Daunt, *ibid.* 49, 435 (1974).
[6]D. P. Grimmer and K. Luszcynski, J. Low Temp. Phys. 26, 19 (1977).
[7]B. P. Cowan, M. G. Richards, A. L. Thomson, and W. J. Mullin, Phys. Rev. Lett. 38, 165 (1977).
[8]M. G. Richards, Proceedings of the International Quantum Crystals Conference, Colorado State University, Fort Collins, 1977 (unpublished).
[9]K. Carneiro, W. D. Ellenson, L. Passell, J. P. McTague, and H. Taub, Phys. Rev. Lett. 37, 1695 (1976).
[10]M. Nielsen, J. P. McTague, and W. Ellenson, J. Phys. (Paris) 38, C 4–10 (1977).
[11]M. Bretz, Ph.D. dissertation (University of Washington (1971) (unpublished); Phys. Rev. Lett. 31, 1447 (1973).
[12]J. A. Herb and J. G. Dash, Phys. Rev. Lett. 29, 846 (1972).
[13]G. J. Goellner, J. G. Daunt, and E. Lerner, J. Low Temp. Phys. 21, 347 (1975).
[14]M. Bretz and S. Polanco, in *Proceedings of the Fourteenth International Conference on Low Temperature Physics*, edited by M. Krusius and M. Vuorio (North-Holland, Amsterdam, 1975), Vol. 1, p. 451; Phys. Rev. B 17, 151 (1978).
[15]Trademark, Union Carbide Corp. Carbon Products Division. Grafoil is a large-area commercially available form of exfoliated graphite.
[16]S. W. Van Sciver, Phys. Rev. B 18, 277 (1978).
[17]S. W. Van Sciver in Ref. 14, p. 368.
[18]C. N. Koutsogeorgis and J. G. Daunt (unpublished).
[19]S. B. Crary and O. E. Vilches, Phys. Rev. Lett. 38, 973 (1977).
[20]S. B. Crary, O. Ferreira, and O. E. Vilches, International Quantum Crystals Conference, Colorado State University, Fort Collins, 1977 (unpublished). This post deadline paper is available from one of us (O.E.V.).
[21]Recent calculations show ^{3}He not to have a bound state in 2-D. See A. D. Novaco and C. E. Campbell, Phys. Rev. B 11, 2525 (1975); and M. D. Miller and L. H. Nosanow (unpublished). Earlier calculations had predicted very weak binding. See R. H. Anderson and T. C. Foster, Phys. Rev. 151, 190 (1966); A. Bagchi, Phys. Rev. A 3, 1133 (1971).
[22]R. L. Siddon and M. Schick, Phys. Rev. A 9, 907 (1974).
[23]R. L. Siddon and M. Schick, Phys. Rev. A 9, 1753 (1974).
[24]M. Bretz, Phys. Rev. Lett. 38, 501 (1977).
[25]S. V. Hering, S. W. Van Sciver, and O. E. Vilches, J. Low Temp. Phys. 25, 793 (1976).
[26]J. G. Dash (unpublished).
[27]R. L. Elgin, D. L. Goodstein, and J. Greif (private communication).
[28]S. V. Hering, Ph.D. thesis, (University of Washington, 1974) (unpublished).
[29]A. D. Novaco, Phys. Rev. B 13, 3194 (1976).
[30]L. M. Sander, M. Bretz, and M. Cole, Phys. Rev. B 14, 61 (1976).